Design of Synthetic 3-D Pulmonary Phantoms using 2-D Graphical User Interface

Arijit De[1] , Nirmal Das[1], Ram Sarkar[1], Punam K. Saha[2], Subhadip Basu[1,*]

[1] Department of Computer Science & Engineering, Jadavpur University, Kolkata-700032, India.
[2]Department of ECE and Radiology, University of Iowa, Iowa City, IA 52242, USA
* Corresponding Author: subhadip@cse.jdvu.ac.in

Abstract. Analysis of pulmonary artery or vein tree has utmost importance in the study and clinical diagnosis of Chronic Obstructive Pulmonary Diseases(COPD). Due to difficulty in acquiring real life patient data and highly complex structure of artery/vein tree, design of imitated/approximate digital pulmonary phantoms for experimental purposes is an active research area. In this work, we discuss theory and methods of designing 3-D mathematical phantoms based on real pulmonary data using a custom made Graphical User Interface (GUI). These approximate phantoms are made using 3-D spheres as the basic unit which are placed in 3-D space using cubic Bezier curves. Results and design steps are explained using appropriate 3-D rendering of digital phantoms developed by our GUI.

Keywords: Human pulmonary vasculature; 3-D rendering; digital phantom; mathematical modeling; COPD; Artery; Vein;

1 Introduction

Respiration is an essential process for the survival of living organisms. In case of human beings, it is performed collectively by the nose, nasal cavities, pharynx, larynx, and trachea that divide into bronchi and enters into the lungs where it further subdivides into bronchioles and finally alveoli. Exchange of gases (Oxygen and Carbon dioxide) with the blood vessels takes place in the alveoli of the lungs. The alveoli are tiny air sacs within the lungs where the exchange of oxygen and carbon dioxide takes place.

The pulmonary artery and pulmonary veins carry deoxygenated and oxygenated blood respectively and form a separate circuit through the heart and lungs only. These arteries and veins are intertwined along the air ways and branches successively until they form capillaries in the alveolar region.

The airways keep on branching until very fine alveoli are formed. This branching has an order of 17 according to [1] and the lowest order has endings in the order of 10^9. Pulmonary arteries and veins run along the surface of these fine structures. All these give us an idea of the complexity of the artery/vein (A/V) network in human lungs.

Analysis of pulmonary vessel network is very important for diagnosis of several diseases related to lungs. Chronic Obstructive Pulmonary Diseases (COPD) are a group of diseases that blocks airflow inside the lungs and make it difficult to breathe [2]. Emphysema and chronic bronchitis are the most common conditions that make up COPD. Pulmonary Embolism (PE) is another disease in which one or more arteries/veins in the lungs get blocked. In most cases, PE is caused by blood clots that

travel to the lungs from the legs or, rarely, from other parts of the body (deep vein thrombosis). The symptoms include difficulty in breathing, chest pain and cough (sometimes accompanied by blood) [3].

With the help of clearly distinct artery and vein regions in 3-D images of pulmonary vessels, diagnosis on patients will be more efficient and fast as embolisms or any unusual structures can be accurately identified.

Segmented pulmonary arteries and veins from patients' *in-vivo* chest images (CT Scan/Ultrasound etc.) have useful clinical applications in COPD [4]. It is the first step towards further analysis like flow analysis [5] of the vessel network for detection of any obstruction (in case of PE).

Due to high branching factor and large number of bifurcated or intertwined vessels, *in-vivo* analysis of pulmonary A/V tree is a complex and time-consuming process and needs to be handled by domain experts. Also, to get different kinds of real data, many human patients are required but the repeated exposure to CT scan/MRI is harmful. Hence, the need to have *prototype* or *synthetic* structures arises as this will reduce the dependency on participation of patients during diagnosis. These synthetic structures generated mathematically are called *phantoms* which are smaller and relatively simpler than real pulmonary A/V trees, while maintaining the same structural features like bifurcations, intertwinements and conjointness. This type of phantoms is called approximate phantoms. There are two types of phantoms in general – 1) physical and 2) digital. Physical phantoms are created by casting a replica of actual vasculature. For example, pig lung cast phantom is generated by injecting a rapid hardening compound into the pulmonary vasculature extracted by performing pneumonectomy on the ensanguined pig. Then the vessel cast is digitized using a CT scanner. Both synthetic and physical phantoms were used in [6–9] for experimentation and analysis. Digital phantoms are made by creating multiple tubular structures of varying geometry and various scales of overlap and attaching them at desired points so as to mimic the actual structure. Both types of phantoms are used for assessing performance of segmentation of pulmonary A/V tree, qualitatively and quantitatively. Different types of physical vessel phantoms are in use, for quantitative assessment of mean differences between the clinical studies and the phantom-based experiments as stated in [10–12].

In many theoretical studies, physical phantoms are not essential rather approximate digital phantoms fulfill the basic purposes. Hence, several researchers have paid attention to the development of synthetic vascular phantoms. In order to efficiently test new algorithms and experiment on pulmonary data, the size and complexity of the data can be reduced keeping the structural features like branching angle, width of vessels intact or scaled to a lower resolution for fast computation.

The main purpose of our work is to recreate the vascular structures in the digital space, using mathematical curve generation techniques and 3-D graphical rendering. In contemporary literature , a number of research articles are available on digital phantom generation [10–13] and computational analysis of blood vessels [14–16]. Most of the research works conducted previously focuses on coronary arteries and myocardial infarction as seen in [10, 12]. But substantial work on digital phantom generation of pulmonary vasculature is not available yet, hence our work is focused on pulmonary A/V which have a higher degree of complexity due to repeated bifurcations. A different approach in phantom generation is shown in [13] that applies computer generated 3-D mesh for creating vascular structures. But in this present work, we have used 3-D spheres as the building blocks of vessels. The works in [14, 15] focuses on centrelines of carotid arteries.

From the above discussion, the importance of mathematically generated synthetic 3D phantoms have been clearly established. The phantom generation method of the

present work is aligned with the work [17][18] but the previous methods concentrated on generating cerebrovascular phantom. The present work discusses about generation of approximate mathematical phantom mimicking real pulmonary A/V network (conjointness of artery-vein at varying scale) and reconstructing accurate pulmonary phantom with the help of a custom-developed GUI. In this GUI, we can select points from a real lung image data and create small portions of the entire lung network having similar curvature and width. This tool will also be useful to the research community to prepare ground truth images of pulmonary data.

2 Theory and method

A 3-D cubic grid is expressed by $\{\mathcal{Z}^3 | \mathcal{Z}\ is\ the\ set\ of\ positive\ integers\}$. A point on the grid, which is frequently referred as a voxel, is a member of $\mathcal{Z}^3$ and is denoted by a triplet of integer coordinates. Each voxel has 26 adjacent voxels, i.e. two voxels $A = (x_1, x_2, x_3)$ and $B = (y_1, y_2, y_3) \in \mathcal{Z}^3$ are adjacent if and only if

$$\{\max(|x_i - y_i|) \leq 1 | \ 1 \leq i \leq 3 \},$$

where $|\cdot|$ means the absolute value. Two adjacent points in a cubic grid are often referred to as neighbors of each other. All 26 neighbors of a voxel $\mathcal{V}$ omitting itself are symbolized as $\mathcal{N}^*(\mathcal{V})$.

2.1 Distance Transform

The distance transform (DT) is an algorithm generally applied to binary images. The output of this algorithm is same as the input image except that the values of each foreground points of the image are changed to the distance to the nearest background from that point. Numerous DT algorithms have been developed both in 2-D and 3-D [19–22] in the past. If $P = (x_1, x_2, x_3)$ is a point in a 3-D image, then DT value of that point will be,

$$DT(P) = \begin{cases} DT(Q_i) + d_k, & | \ DT(Q_i) + d_k < DT(P) \\ DT(P), & | \quad otherwise \end{cases} \quad (1)$$

where, Q_i is the neighbor of P, i =1, 2, . . ., 26 and $d_{k=1,2,3}$ is the approximate Euclidean distance from three different kinds of neighbor. Distance transform performs very well in case of binary images.

2.2 Phantom generation

We now define a sphere $\mathcal{S}(o, r)$, with the center o having coordinates (x_c, y_c, z_c) and radius r is the locus of all points (x, y, z) in $\mathcal{Z}^3$ such that

$$(x + x_c)^2 + (y + y_c)^2 + (z + z_c)^2 = r^2 \quad (2)$$

The points on the sphere with radius r can be parameterized via, $x = x_0 + rcos\theta sin\gamma$, $y = y_0 + rcos\theta sin\gamma$, $z = z_0 + rcos\gamma$, where $0 \leq \theta \leq 2\pi$ and $0 \leq \gamma \leq \pi$.

Two points p_1 and p_2 in $\mathcal{Z}^3$ may be connected by a set of adjacent points $\{p_1, p_2, \dots, p_i, p_{i+1}, \dots, p_n\}$. Then a tubular structure $T(p_1, p_n)$ in $\mathcal{Z}^3$ having uniform radius r may be defined as a collection of spheres $\mathcal{S}_1, \dots \mathcal{S}_i, \mathcal{S}_{i+1}, \dots, \mathcal{S}_n$ having radius r and the set of adjacent center points, $C = \{p_1, p_2, \dots, p_i, p_{i+1}, \dots, p_n\}$ respectively. When the points p_1 and p_n are connected through a digital straight line then the corresponding tubular structure forms a simple tubular structure or *pipe* as shown in Fig. 1(a). One or more *pipes* may be joined together to form other shapes as shown in Fig. 1(b) and Fig. 1(c).

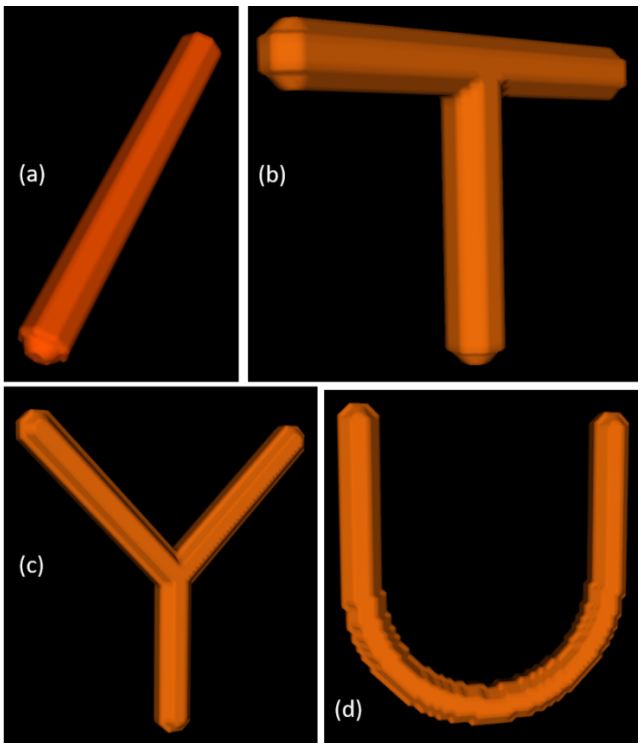

Fig 1 3-D rendering of some basic shapes like (a) straight tube, (b) T-Shape, (c) Y-Shape and (d) U-Shape

The T-Shape, which is shown in Fig. 1(b), is generated by first creating a straight tube as shown in Fig. 1(a) and then placing equal number of spheres from one end of the tube extending at right angle to the first tube. The Y-Shape, which is shown in Fig. 1(c), is created by joining three simple straight tubes at a common end keeping two of them at 135° from the vertical tube. The U-Shape, as shown in Fig. 1(d), is prepared by first creating two parallel straight tubes at a known distance from each other. Then, a half-circle is created using the general equation of a circle and placing

the sphere centers in the locus of the equation in such a way such that the ends of the half-circle coincide with the ends of the tubes.

For phantom design in this work, piecewise linear interpolation technique using cubic *Bézier curves* has been used. To develop pulmonary A/V trees, multiple tubular structures are generated branching at various locations. A *Bezier curve* is a parametric curve that uses *Bernstein Polynomial* as a basis function [23]. A Bézier curve of degree n (order n+1) is represented by $\mathcal{R}(t) = \sum_{i=0}^{n} b_i \mathcal{B}_{i,n}(t), 0 \leq t \leq 1$. The coefficients b_i, called the control points or Bezier points, together with the basis function $\mathcal{B}_{i,n}(t) = \sum_{i=0}^{n} {}_{i}^{n}C(1-t)^{n-i}t^{i}b_i$ determine the shape of the curve.

Two tubular structures $T_1(u_1, u_n); u_1, u_n \in C_1$ and $T_2(v_1, v_m); v_1, v_m \in C_2$ in $\mathcal{Z}^3$, may be connected to each other when, $C_1 \cap C_2 \neq \emptyset$.

An example of a conjoint structure made of two curved tubular structures which is a common case in real pulmonary artery/vein tree is given in Fig. 2(a). The cross section at the conjoint region which depicts the degree of conjointness is shown in Fig. 2(b).

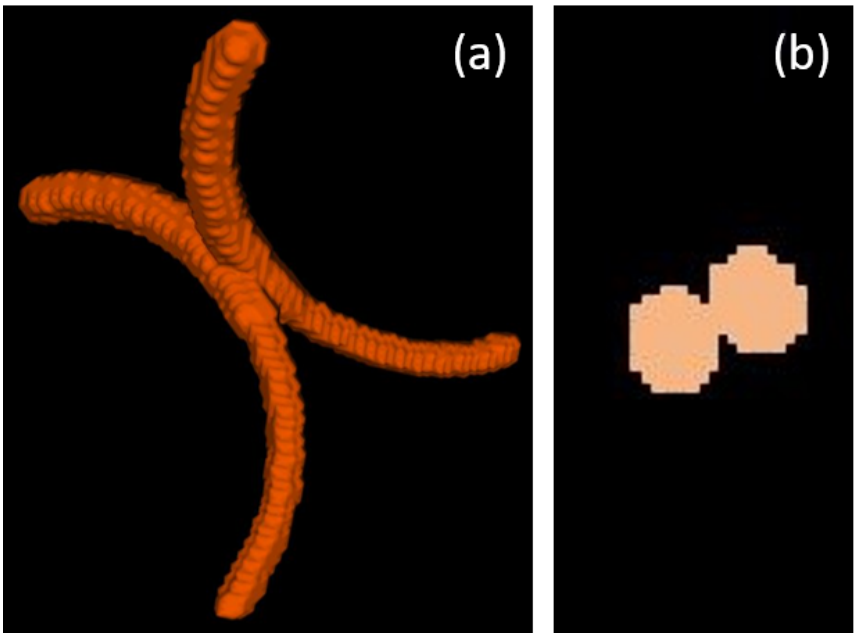

Fig 2 (a) 3-D rendered diagram of two curved pipes joined together, (b) Cross section at the conjoint region

In tubular structure $T(p_1, p_n)$ in $\mathcal{Z}^3$, the spheres at the endpoints may have different radii which are calculated by the Euclidean distance transform (DT) value of the image as it approximately represents the distance of the voxel from the surface of the object. The radius of the spheres is gradually decreased from r_1 to r_n by the following methodology. We define *range* as the number of centre points. We define another variable *step* as

$$step = range \div (r_1 - r_n) \quad (3)$$

The radius decreases by 1 after every $step$ iterations until its value becomes r_n. An illustration of the said concept is shown in Fig. 3.

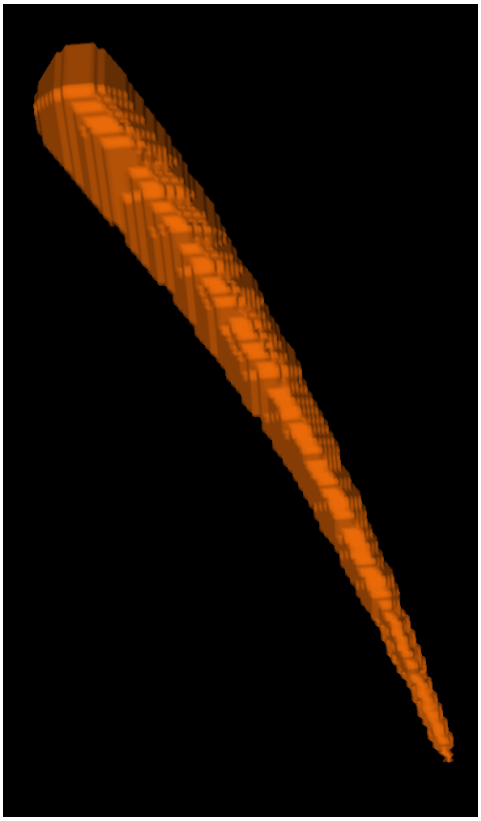

Fig 3 A curved pipe with varying diameter

In this work, the phantoms have been designed and saved in analyze image formats which are widely used in medical imaging field and easily visualized using itk-SNAP Version 3.6.0 [24, 25].

As shown in Fig. 3, such pipes with varying shapes and scales can be assembled together to form a complex structure mimicking that of pulmonary vasculature. In general, the scale varies from thicker vessels which gradually change to thinner vessels as the length increases. The vessels are mostly attached together in higher scale, i.e., when they are thick. Some vessels may overlap one another or meet at lower scale but two or more vessels are not attached at the end. Some complex shapes created based on the said theories are shown in Fig. 4.

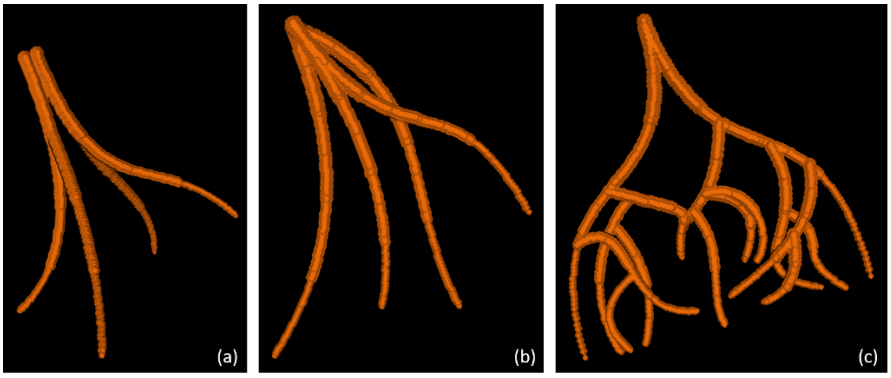

Fig 4 3-D rendering of complex structures created by joining pipes mathematically generated using *Bézier curves*. (a) a structure made of 4 curved pipes joined at one end. (b) are for pipes of varying radii emanating from one point. (c) structure made of several pipes of varying sizes and diameters joined at several points.

3 Experimental Outcomes

We have developed a custom GUI using Qt version 5 [26] which is an open source cross-platform application development framework based on C++ language. It is widely used to develop GUI based applications and also for mobile applications. The output of the generated phantom is shown using itk-SNAP [24, 25] which has impressive 3-D rendering capability.

In this work, we have taken a physical pig lung phantom and generated a digital phantom by replicating a very small portion of the original phantom. It is done by loading the original phantom image in the custom-made GUI and selecting points from the top, front and side view images of the phantom. For each curve, exactly four points need to be selected as we have used cubic Bézier curves which has one start point, one end point and two control points.

Experts can select regions of interest from the original data which can then be mimicked as a mathematically generated digital phantom using the developed software on which various analysis and experiments can be performed. Fig. 5 shows a screenshot of the developed GUI in which the DT of the image is visible and a point is selected.

The curves are generated step by step by adding four points of each curve. The user can generate output at any time and check if the desired phantom is achieved or not. More curves can be added to the current phantom being generated until the desired output is observed. Fig. 6(a - g) shows 12 steps of the pig lung phantom being generated.

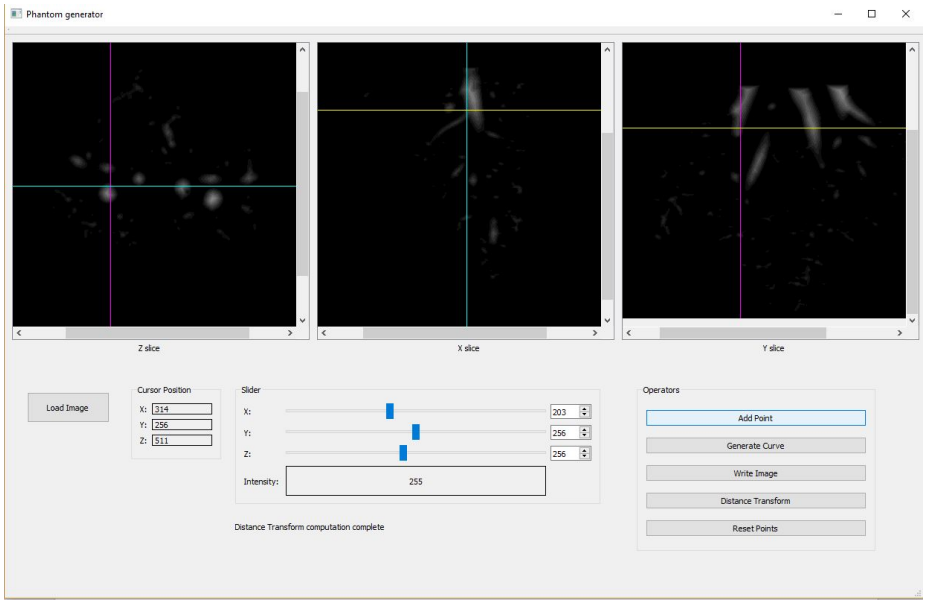

Fig 5 Screenshot of the developed GUI showing basic functionalities like calculating DT, adding points for curve, generating and finally writing the output to disk.

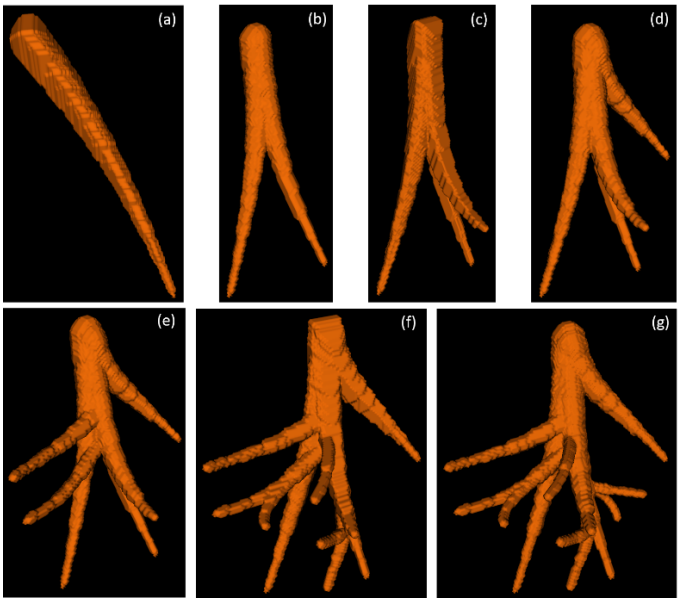

Fig 6 Steps of phantom generation - (a) Step 1, (b) Step 2, (c) Step 3, (d) Step 4, (e) Step 6, (f) Step 10, (g) Step 12

The final phantom which is generated after adding subsequent curves to the phantom in Fig. 6(g), is shown in Fig. 7(b). The region in the physical pig lung phantom, from which the digital phantom is generated is displayed in Fig. 7(a).

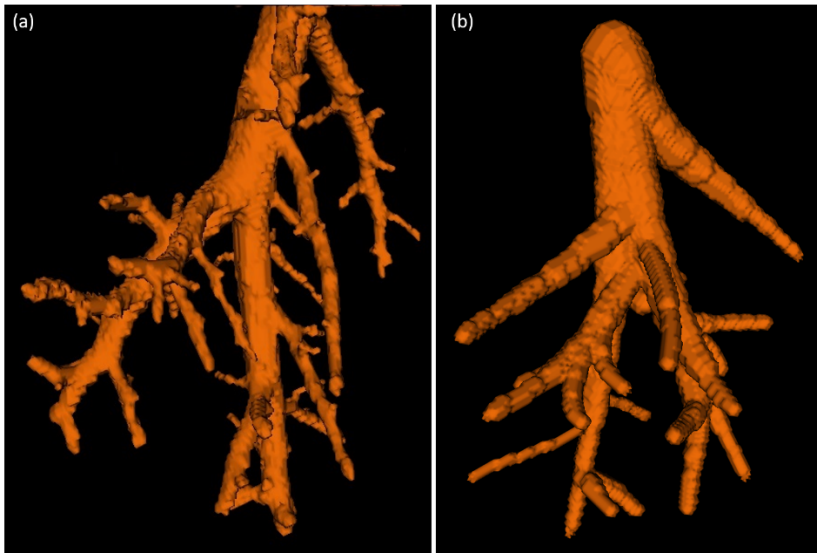

Fig 7 (a) A small region of physical pig lung phantom, (b) digital phantom of the same region generated by our method

Conclusion

In this work, we have generated a near accurate phantom by selecting points from the original data with a user-friendly GUI. As discussed earlier, the purpose of this work is to provide aid in research efforts towards developing digital pulmonary phantoms. This type of digital pulmonary phantoms can be used for analysis of pulmonary lung diseases where segmentation of pulmonary arteries and veins are required.

As these phantoms are smaller in size but structurally similar to real data, results obtained by using these digital phantoms will be very similar or even completely accurate to those obtained using real pulmonary data. Our method requires user intervention for selecting 4 points for each curve which may become a lengthy task in case of generating a complex phantom with many tubes. In the future, automatic detection and segmentation of pulmonary arteries and veins of varying scale can be facilitated using phantoms developed by our method.

Acknowledgement

This project is partially supported by the CMATER research laboratory of the Computer Science and Engineering Department, Jadavpur University, India, DST PURSE-II and UPE-II project and Research Award (F.30-31/2016(SA-II)) from UGC, Government of India, Government of India.

References

1. Singhal S, Henderson R, Horsfield K, et al (1973) Morphometry of the Human Pulmonary Arterial Tree. Circ Res 33:190–197 . doi: 10.1161/01.RES.33.2.190
2. Murphy TF, Sethi S (2002) Chronic Obstructive Pulmonary Disease. Drugs Aging 19:761–775 . doi: 10.2165/00002512-200219100-00005
3. Fletcher M, Upton J, Taylor-Fishwick J, et al (2011) COPD uncovered: an international survey on the impact of chronic obstructive pulmonary disease [COPD] on a working age population. BMC Public Health 11:1–13 . doi: 10.1186/1471-2458-11-612
4. Gurney JW, Jones KK, Nelson J, et al Thoracic of Emphysema□: in Unselected. i:457–463
5. Das N, Rakshit P, Nasipuri M, Basu S (2017) 3-D Digital flows in cerebrovascular phantoms. In: 9th International conference on Pattern Recognition[ICAPR-2017]. ISI, Bangalore
6. Zhiyun Gao, Grout RW, Holtze C, et al (2012) A New Paradigm of Interactive Artery/Vein Separation in Noncontrast Pulmonary CT Imaging Using Multiscale Topomorphologic Opening. IEEE Trans Biomed Eng 59:3016–3027 . doi: 10.1109/TBME.2012.2212894
7. Cai Z, Bai E (2010) A Dynamic Arterial Tree Phantom for studies of bolus chasing CT Angiography Robert McCabe CIRS Tissue Simulation and Phantom Technology , Ge Wang Madhavan Lakshmi Raghavan and Jarin Kratzberg. 4:88–100
8. Saha PK, Gao Z, Alford SK, et al (2010) Topomorphologic separation of fused isointensity objects via multiscale opening: separating arteries and veins in 3-D pulmonary CT. IEEE Trans Med Imaging 29:840–51 . doi: 10.1109/TMI.2009.2038224
9. Saha PK, Basu S, Hoffman EA (2016) Multiscale Opening of Conjoined Fuzzy Objects: Theory and Applications. IEEE Trans Fuzzy Syst 24:1121–1133
10. Brunette J, Mongrain R, Ranga A, Tardif J-C (2011) An Atherosclerotic Coronary Artery Phantom for Particle Image Velocimetry. Proc Can Eng Educ Assoc 2:
11. Le Floc'h S, Cloutier G, Finet G, et al (2010) On the potential of a new IVUS elasticity modulus imaging approach for detecting vulnerable atherosclerotic coronary plaques: In vitro vessel phantom study. Phys Med Biol 55:5701–5721 . doi: 10.1088/0031-9155/55/19/006
12. Hansen HHG, Lopata RGP, De Korte CL (2009) Noninvasive carotid strain imaging using angular compounding at large beam steered angles: Validation in vessel phantoms. IEEE Trans Med Imaging 28:872–880 . doi: 10.1109/TMI.2008.2011510
13. De Santis G, De Beule M, Van Canneyt K, et al (2011) Full-hexahedral structured meshing for image-based computational vascular modeling. Med Eng Phys 33:1318–1325 . doi: 10.1016/j.medengphy.2011.06.007
14. Piccinelli M, Veneziani A, Steinman DA, et al (2009) A framework for geometric analysis of vascular structures: Application to cerebral aneurysms. IEEE Trans Med Imaging 28:1141–1155 . doi: 10.1109/TMI.2009.2021652
15. Antiga L, Piccinelli M, Botti L, et al (2008) An image-based modeling framework for patient-specific computational hemodynamics. Med Biol Eng Comput 46:1097–1112 . doi: 10.1007/s11517-008-0420-1
16. Zhu H, Ding Z, Piana RN, et al (2009) Cataloguing the geometry of the human coronary arteries: A potential tool for predicting risk of coronary artery disease. Int J Cardiol 135:43–52 . doi: 10.1016/j.ijcard.2008.03.087
17. Banerjee A, Dey S, Parui S, et al (2013) Design of 3-D Phantoms for Human Carotid Vasculature. In: 2013 Third International Conference on Advances in Computing and Communications. IEEE, pp 347–350
18. Banerjee A, Dey S, Parui S, et al (2013) Synthetic reconstruction of human carotid vasculature using a 2-D / 3-D interface. Icacci 60–65
19. Borgefors G (1986) Distance transformations in digital images. Comput vision, Graph image Process 34:344–371
20. Borgefors G (1984) Distance transformations in arbitrary dimensions. Comput Vision, Graph Image Process 27:321–345 . doi: 10.1016/0734-189X(84)90035-5
21. Danielsson PE (1980) Euclidean distance mapping. Comput Graph Image Process

14:227–248 . doi: 10.1016/0146-664X(80)90054-4
22. Cuisenaire O, Macq B (1999) Fast Euclidean Distance Transformation by Propagation Using Multiple Neighborhoods. 76:163–172
23. Abrahamsen A (2000) Cubic B ` ezier Curves. Control 1–4
24. Paul Y, Guido G (2006) itk-SNAP
25. Yushkevich PA, Piven J, Hazlett HC, et al (2006) User-guided 3D active contour segmentation of anatomical structures: significantly improved efficiency and reliability. Neuroimage 31:1116–1128
26. Company TQ, Project Q (2006) Qt Project